J Mol Model (2007) 13:1017–1025
DOI 10.1007/s00894-007-0213-8

ORIGINAL PAPER

On the relative stabilities of the alkali cations 222 cryptates in the gas phase and in water-methanol solution

Elisa S. Leite · Sidney R. Santana · Philippe H. Hünenberger · Luiz C. G. Freitas · Ricardo L. Longo

Received: 6 January 2007 / Accepted: 27 April 2007 / Published online: 14 July 2007

Abstract The relative stabilities of the alkali $[M \subset 222]^+$ cryptates (M = Na, K, Rb and Cs) in the gas phase and in solution (80:20 v/v methanol:water mixture) at 298 K, are computed using a combination of ab initio quantum-chemical calculations (HF/6-31G and MP2/6-31+G*//HF/6-31+G*) and explicit-solvent Monte Carlo free-energy simulations. The results suggest that the relative stabilities of the cryptates in solution are due to a combination of steric effects (compression of large ions within the cryptand cavity), electronic effects (delocalization of the ionic charge onto the cryptand atoms) and solvent effects (dominantly the ionic dessolvation penalty). Thus, the relative stabilities in solution cannot be rationalized solely on the basis of a simple match or mismatch between the ionic radius and the cryptand cavity size as has been suggested previously. For example, although the $[K \subset 222]^+$ cryptate is found to be the most stable in solution, in agreement with experimental data, it is the $[Na \subset 222]^+$ cryptate that is the most stable in the gas phase. The present results provide further support to the notion that the solvent in which supramolecules are dissolved plays a key role in modulating molecular recognition processes.

Keywords Molecular recognition · Supramolecular chemistry · Ab initio quantum chemistry · Monte Carlo simulation · Cryptates · Solvent effects · Complexation selectivity

Electronic supplementary material The online version of this article (doi:10.1007/s00894-007-0213-8) contains supplementary material, which is available to authorized users.

E. S. Leite · S. R. Santana · R. L. Longo (✉)
Departamento de Química Fundamental,
Universidade Federal de Pernambuco,
50740-540 Recife, PE, Brazil
e-mail: longo@ufpe.br

E. S. Leite · L. C. G. Freitas
Departamento de Química,
Universidade Federal de São Carlos, CP-676,
13565-905 São Carlos, SP, Brazil

P. H. Hünenberger
Laboratory of Physical Chemistry, ETH,
8093 Zurich, Switzerland

Introduction

Molecular recognition plays a key role in many biochemical processes, in the design of new materials, and in the development of new procedures for analytical chemistry [1–7]. Host-guest interactions, which are usually non-covalent, have been modeled in many simple systems using the premises of supramolecular chemistry. Some examples of recently modeled host-guest interactions are the inclusion of substituted benzenes donor compounds in the tetracationic host cyclobis(paraquat-p-phenylene) [8], alkali cations in calixarenes [9], metals in the {2}-gallium cryptand [10], $CDCl_3$ in the β-cyclodextrin [11], amines in calixarenes [12], and halogenenbenzoic acids in the α-cyclodextrin [13].

The 222 cryptand (Fig. 1) is a synthetic macrocyclic multidentate ligand (host) that exhibits high selectivity towards metal ions (guests), and has been used as a prototype for molecular recognition by complexation (formation of a cryptate) [1]. In addition, 222 cryptate formation bears some analogy with the action of valinomycin, a macrocyclic molecule highly selective for potassium ions over sodium ions within the cell membrane. The potassium-valinomycin complex is about a thousand times

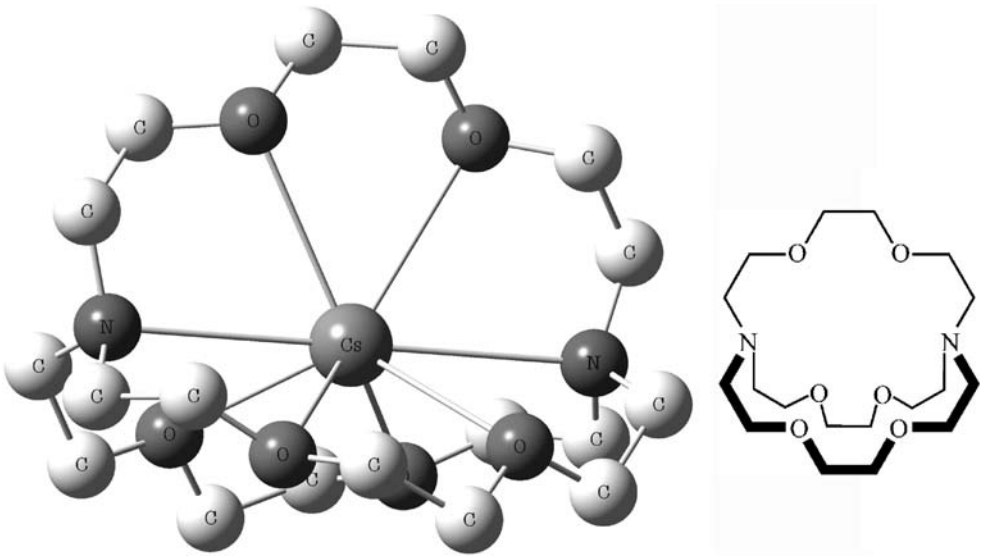

Fig. 1 Optimized geometry at the HF/LanL2DZ(Cs)-6-31+G* (cryptand) level of the *endo* [Cs ⊂ 222]$^+$ cryptate in the gas phase and schematic representation of the 222 cryptand. Hydrogen atoms have been omitted for clarity. The structures of the other cryptates are provided in Figs. S1, S2, S3, S4, S5, S6 (supplementary material)

more stable than the sodium-valinomycin complex. This difference is important for maintaining the selectivity of valinomycin towards the transport of potassium ions in biological systems [14, 15].

Solvent effects have been claimed to play an essential role in determining the relative stabilities of the alkali cations 222 cryptates [16–18], as well as those of other ionophores, macrocyclic complexes and biochemical complexes in solution [19]. These solvent effects have been properly accounted for in previous explanations of the selectivity of specific crown ethers [20, 21] and cryptands [22, 23] towards alkali ions. However, they are still being overlooked in the interpretation of some experimental data [24–26] involving cryptates. For instance, the selectivity of the 222 cryptand towards the K^+ cation in the alkali series is often explained solely on the basis of a comparison between the (estimated) cavity radius of the cryptate and the corresponding ionic radii (cavity match or mismatch) [24], disregarding a possible influence of the solvent. In addition, the cryptand flexibility makes its cavity radius determination by geometrical methods difficult and ambiguous, so that model chemical equations, such as, $\left[M(H_2O)_6\right]^+ + [222] \rightarrow [M \subset 222]^+ + 6H_2O$, have been developed to overcome this difficulty [27].

The main goal of the present work is to improve upon this (simplistic) interpretation by quantifying solvent effects on the relative stabilities of the [M ⊂ 222]$^+$ cryptates (M = Na, K, Rb and Cs) in a 80:20 (v/v) methanol:water solution. This is done using theoretical computational methods in a similar spirit as previous work considering alkali crown ether complexes in water [19, 20]. The present study combines results of two different approaches: gas phase ab initio quantum-chemical calculations (to estimate gas-phase affinities) and explicit-solvent Monte Carlo free-energy calculations (to evaluate solvation free energies). The [M ⊂ 222]$^+$ cryptates are particularly well suited for such a theoretical investigation, due to the availability of structural [27, 28] and thermodynamical [29] data, and the existence of previous theoretical results [16, 18, 22, 23, 30]. Furthermore, these compounds are quite rigid compared to other ionophores, which significantly reduces the requirement for conformational sampling during the quantum-chemical and free-energy calculations.

Methods

The thermodynamic cycle involving the cryptate formation reactions in the gas phase and in the methanol-water solution reads

$$\begin{array}{ccccc} 222(sol) & + & M^+(sol) & \xrightarrow{\Delta_c G^\circ\,(M)} & [M\subset 222]^+(sol) \\ \downarrow -\Delta_{sol}G^\circ\,(222) & & \downarrow -\Delta_{sol}G^\circ\,(M^+) & & \uparrow \Delta_{sol}G^\circ\,([M\subset 222]^+) \\ 222(g) & + & M^+(g) & \xrightarrow[\Delta_g G^\circ\,(M)]{} & [M\subset 222]^+(g) \end{array} \quad (1)$$

It involves the standard Gibbs free energies of complexation in the gas phase $\Delta_g G°(M)$ and in solution $\Delta_c G°(M)$, as well as the Gibbs solvation free energies of the cryptand $\Delta_{sol}G°(222)$, of the alkali cation $\Delta_{sol}G°(M^+)$, and of the cryptate $\Delta_{sol}G°([M \subset 222]^+)$. The standard states correspond to an ideal gas at a pressure of 1 bar (gas-phase

species) and an ideal solution at a concentration of 1 mol L^{-1} (solvated species). These quantities are related through

$$\Delta_c G^\circ(M) = \Delta_g G^\circ(M) - \Delta_{sol} G^\circ(222) - \Delta_{sol} G^\circ(M^+) + \Delta_{sol} G^\circ\left([M \subset 222]^+\right). \quad (2)$$

The difference between the free energies of complexation for two cryptates $[M \subset 222]^+$ and $[N \subset 222]^+$ in solution

$$\Delta\Delta_c G(M \to N) = \Delta_c G^\circ(N) - \Delta_c G^\circ(M) \quad (3)$$

is then given by

$$\begin{aligned}\Delta\Delta_c G(M \to N) &= [\Delta_g G^\circ(N) - \Delta_g G^\circ(M)] \\ &\quad - [\Delta_{sol} G^\circ(N^+) - \Delta_{sol} G^\circ(M^+)] \\ &\quad + [\Delta_{sol} G^\circ([N \subset 222]^+) \\ &\quad - \Delta_{sol} G^\circ([M \subset 222]^+)] \\ &= \Delta\Delta_g G(M \to N) \\ &\quad - \Delta\Delta_{sol} G^{ion}(M^+ \to N^+) \\ &\quad + \Delta\Delta_{sol} G^{cry}([M \subset 222]^+ \to [N \subset 222]^+)\end{aligned} \quad (4)$$

Note that the three "ΔΔ" quantities do not depend on the choice of standard states. The quantity $\Delta\Delta_g G$ represents the difference in gas-phase complexation free energies between the ions considered, while the quantities $\Delta\Delta_{sol} G^{ion}$ and $\Delta\Delta_{sol} G^{cry}$ represent changes in solvation free energies upon "mutating" one ion into the other (either isolated in solution or within the solvated cryptand). These quantities were calculated as described below.

The gas phase free-energy difference $\Delta\Delta_g G$ in Eq. (4) is defined as

$$\Delta\Delta_g G(M \to N) = \Delta_g G^\circ(N) - \Delta_g G^\circ(M) \quad (5)$$

Expressing $\Delta_g G^\circ$(M) in terms of the corresponding changes in internal energy, pressure-volume energy, and entropy gives,

$$\Delta_g G^\circ(M) = \Delta_{g,0} E(M) + \Delta\Delta_{g,T} E(M) - RT - T\Delta S^\circ_{g,T}(M) \quad (6)$$

where $\Delta_{g,0}E$ is the internal energy change at $T = 0$ K, $\Delta\Delta_{g,T}E$ a thermal correction to this change from T=0 to 298 K (related to the heat capacities of the involved species), R the ideal gas constant (the third term accounts for the standard pressure-volume work of the reaction) and $\Delta S^\circ_{g,T}$ the standard entropy change at $T = 298$ K.

All quantities involved in Eq. (6) were calculated using ab initio quantum chemical methods together with the rigid-rotor and harmonic-oscillator approximations [31]. These gas-phase calculations were performed with the Gaussian 98 program [32], using its default parameters and convergence criteria.

To initiate the calculations for the different cryptates, the crystallographic structure of the $[Na \subset 222]^+$ cryptate [28], which is close to the D_3 symmetry, was fully optimized without any symmetry constraints at the HF/6-31+G* level. The choice for not imposing symmetry constraints was to avoid a bias toward any local minimum (C_1, C_s, C_3 and D_3). It should be noted, however, that the optimized structure has a D_3 symmetry up to 1 pm. This optimized structure was then used as the starting geometry for the $[K \subset 222]^+$, $[Rb \subset 222]^+$ and $[Cs \subset 222]^+$ cryptates, which were also fully optimized at the HF level. The resulting structure is depicted in Fig. 1 for the $[Cs \subset 222]^+$ complex.

The electronic energies were calculated based on these structures at the MP2 level [33] and corrections for basis-set superposition errors (BSSE) were included using the counterpoise approach [34]. For both geometry optimization (HF level) and energy calculation (MP2 level), an all-electron 6-31+G* basis set was used for the Na and K atoms, while the quasi-relativistic effective core potential (ECP) LanL2DZ basis set [21, 35] was employed for the K (second calculation), Rb and Cs atoms (retaining the 6-31+G* representation for the cryptand, whenever present). The all-electron basis set result was used for K when considering the transformation Na → K, whereas the ECP basis set result was employed for the K → Rb transformation. To convert the calculated energies into free energies, the entropy contributions and thermal corrections were evaluated at the HF level with a basis set reduced from 6-31+G* to 6-31G (cryptand and metal, unless using ECP) using vibrational frequencies scaled by 0.8929 [33].

The solvation free energy differences $\Delta\Delta_{sol} G^{ion}$ and $\Delta\Delta_{sol} G^{cry}$ in Eq. (4) were calculated using the thermodynamic integration method [36], based on explicit-solvent Monte Carlo (MC) simulations at constant temperature and pressure. These calculations were performed with rigid geometries for the cryptand and solvent molecules (no intramolecular potential energy terms). The intermolecular potential energy consisted of a sum of atom-based van der Waals and electrostatic interaction terms described by the Lennard-Jones [37] and truncated Coulomb plus reaction-field [38] potentials, respectively.

The Lennard-Jones parameters for the ions and the cryptand atoms were taken from the OPLS force field [39]. The charges of the isolated ions were set to $+1e$. Partial charges for the cryptate atoms were obtained by application of the CHELPG procedure [40] to electrostatic potentials from the ab initio calculations at optimized geometries (see above), with the Breneman radii for the alkali atoms set to their corresponding ionic radii [41]. The CHELPG analysis was performed at the same level of theory as the optimization for $[Na \subset 222]^+$ and $[K \subset 222]^+$, or at the HF/6-31G level with an SDD pseudopotential [42] for the Rb and Cs atoms in $[Rb \subset 222]^+$ and $[Cs \subset 222]^+$. The resulting charges are

reported in details in Table S1 (supplementary material) while the main features summarized in Table 1. The internal parameters for water and methanol were taken from the TIP4P and OPLS models [43], respectively.

The MC simulations were performed under periodic boundary conditions based on cubic computational boxes filled with an 80:20 (v/v) methanol:water solution, which was chosen for comparison with available experimental data [29]. For the alkali cations the simulations involved one ion, 320 methanol molecules and 180 water molecules within a box of (initial) edge length 2.94 nm. For the cryptates, they involved one solute, 2560 methanol and 1440 water molecules within a box of (initial) edge length 6.02 nm. All simulations were carried out at 298 K and 1 atm using the DIADORIM program [44], with rigid cryptates in the optimized geometries resulting from the gas phase ab initio calculations (see above). The solvent translational and rotational moves, and the volume variations, were chosen to achieve acceptance ratios of 45%, 45% and 30%, respectively. Electrostatic interactions were truncated using cutoff distances of 0.85 nm (alkali cations) or 1.20 nm (cryptates), and the mean effect of longer-ranged interactions was approximately accounted for by means of a reaction-field correction [38].

For the alkali cations, the $\Delta\Delta_{sol}G^{ion}$ values were obtained from a series of simulations involving the successive changes $Na^+ \rightarrow K^+ \rightarrow Rb^+ \rightarrow Cs^+$. For the cryptates, the corresponding values $\Delta\Delta_{sol}G^{cry}$ were obtained from three series of three consecutive changes involving the discharging of the ion within the solvated cryptate $[M \subset 222]^+ \rightarrow [M \subset 222]$, followed by the change $[M \subset 222] \rightarrow [N \subset 222]$, and completed by the charging process $[N \subset 222] \rightarrow [N \subset 222]^+$. As a result of this decomposition, a complete separation between the electrostatic and van der Waals contributions to the Gibbs free energy changes could be achieved. The evaluation of all above quantities required six independent free-energy simulations. For each transformation, the thermodynamic integration method was applied using a linear λ-coupling scheme, involving independent simulations at 10 equidistant λ-points. Each λ-point involved 4×10^5 MC steps for equilibration and 1×10^6 (alkali cations) or 6×10^5 (cryptates) MC steps of production.

Absolute ionic solvation free energies computed from explicit solvent simulations are notoriously sensitive [45] to the boundary conditions (*e.g.* box shape and size) and treatment of electrostatic interactions (*e.g.* application of cutoff). However, because the corresponding errors arise mostly from an incorrect description of long-range solvation, they are likely to cancel out to a large extent within the quantities $\Delta\Delta_{sol}G^{ion}$ and $\Delta\Delta_{sol}G^{cry}$. To investigate the validity of the present protocol, absolute ionic solvation free energies were also computed for alkali cations in water and in the water-methanol mixture, and compared with experiment. This was done by adding an estimate for the standard absolute solvation free energy $\Delta_{sol}G^{\circ}_{abs}$ of Na^+ to the $\Delta\Delta_{sol}G^{ion}$ values computed for the successive pairs of alkali cations. In practice, the former quantity was obtained from the series of "mutations" $Na^+ \rightarrow Na^0 \rightarrow CH_4 \rightarrow$ *dummy*, as described elsewhere [43].

Table 1 Atomic partial charges (in $|e|$) used in the explicit-solvent MC simulations of the $[M \subset 222]^+$ cryptates, presented in the form of averages over all atoms related by symmetry operations within the D_3 group (see Fig. 1): one metal ion (M), two nitrogen atoms (N) and six oxygen atoms (O)

Atoms	$[Na \subset 222]^+$	$[K \subset 222]^+$	$[Rb \subset 222]^+$	$[Cs \subset 222]^+$
M	0.656	0.682	0.677	0.748
N	−0.266	−0.267	−0.241	−0.274
O	−0.496	−0.515	−0.522	−0.556

Charges on carbon and hydrogen atoms are not reported. The complete list of partial charges used for all atoms is provided in Table S1 (supplementary material).

Results and discussions

The coordinates and structures of the geometry-optimized gas-phase structures of the $[M \subset 222]^+$ cryptates where the alkali cations are enclosed by the cryptand cavity (*endo*) are provided in Tables S2, S3, S4, S5, S6, S7, S8 and Figs. S1, S2, S3, S4, S5 (supplementary material), respectively. These structures were optimized at the HF level of theory using either the (all-electrons) 6-31+G* basis set for Na and K or the (effective core potential) ECP-LanL2DZ basis set for the K (second calculation), Rb and Cs. The corresponding distances of the metal-donor atoms (Metal-Oxygen and Metal-Nitrogen atoms) are reported in Table 2 and energies are reported in Table 3. The calculated structures are in good agreement with the crystallographic ones [27–29], even for the largest Cs^+ ion (Fig. 1) and mainly with the most recent determinations [29]. The root-mean-square deviations between the crystallographic and calculated structures for the metal-donor (N, O) atoms are 0.034, 0.030, 0.027 and 0.022 nm for the Na, K (all-electron basis set), Rb and Cs cryptates, respectively. In agreement with observations made in the context of more flexible systems such as the 18C6 crown ether [21], the present results do not show a significant dependence of the optimized structures upon enlargement of the basis set. Except for the bond distances within the macrocycle, which are slightly shorten. This is expected since the increase of the basis sets improves the description of the occupied molecular orbitals, which usually are bonding orbitals, thus causing a

Table 2 $[M \subset 222]^+$ cryptates distances (in pm) between the metal ion and the donor atoms

Distance	Crystallographic Structure	HF/6-31+G*	HF/LANL2DZ(M) 6-31+G*(cryptand)	HF/6-311++G**
Na–N	275 [28], 306 [29]	290	–	292
Na–O	257 [28], 274 [29]	253	–	254
K–N	287 [28], 301 [29]	297	297	–
K–O	279 [28], 283 [29]	282	282	–
Rb–N	299 [28], 300 [29]	–	302	–
Rb–O	291 [28], 291 [29]	–	291	–
Cs–N	302 [28], 308 [29]	–	312	–
Cs–O	296 [28], 296 [29]	–	303	–

decrease of the bond lengths. So, medium size basis sets are more adequate for Hartree-Fock calculations, and an increase of the basis sets would require the improvement of the *N*-basis description with correlated methods [46].

Classical molecular mechanics results [30] have suggested that the facial (*exo*) structure of the $[Cs \subset 222]^+$ cryptate is more stable than the *endo* one in the gas phase. Based on a geometry optimized structure of the *exo* complex (coordinates and structure in Table S7 and Fig. S6, respectively; supplementary material), this suggestion is not supported by the quantum-mechanical results at the present level of theory (Table 2), the *endo* cryptate being more stable by about 46 kJ mol^{-1}. However, the preferred structure in solution may still differ from the gas-phase one. According to ^{133}Cs NMR measurements [47], both *endo* and *exo* structures are present in solution, the former dominating at equilibrium.

The gas-phase internal energy changes involved in Eq. (6), calculated at the MP2 level of theory for the different cryptates (based on the previously optimized structures and including BSSE corrections), are reported in Table 3 together with the corresponding contributions $E_{g,0}$ from the individual species. The associated thermal corrections $\Delta\Delta_{g,T}E$ and standard entropy changes $T\Delta_{g,T}S°$ are reported in Table 4.

The internal energy changes ($\Delta_{g,0}E + \Delta\Delta_{g,T}E$) are very large and negative, their magnitudes decreasing with increasing ionic radius. The standard volume work contribution, $-RT = -2.48$ kJ mol^{-1}, is constant along the series and essentially negligible. The standard entropy contributions, $-T\Delta_{g,T}S°$, are large and positive. They are dominated by the loss of translational entropy upon binding (Sackur-Tetrode equation), while effects related to the restriction of intramolecular vibrations (positive contribution to $-T\Delta_{g,T}S°$) and to the increase in the moment of inertia (negative contribution to $-T\Delta_{g,T}S°$, magnitude increasing with the ionic mass) of the cryptand upon binding are small. As a consequence, the magnitude of the entropic term varies little along the series of alkali ions. The standard gas-phase free energies of binding $\Delta_g G°$ resulting from this partial enthalpy-entropy compensation are still very large and negative. They also decrease in magnitude with increasing ionic radius. This indicates that in the gas phase (at a standard pressure of 1 bar), all cryptates are stable, the

Table 3 Calculated internal energies of complexation $\Delta E_{g,0}(M)$ at 0 K, Eq. (6), for the $[M \subset 222]^+$ cryptates in the gas phase (based on structures optimized at the HF level, and including BSSE corrections), together with the corresponding contributions $E_{g,0}$ from the individual species at the MP2 level

Ion	$E_{g,0}([M \subset 222]^+)$	$E_{g,0}(M^+(222))$ [e]	$E_{g,0}(222(M^+))$ [f]	$E_{g,0}(222–M^+)$ [g]	$\Delta_{g,0}E(M)$ [h]
Na^+ [a]	−1426.1525	−161.6602	−1264.3127	−1264.2998	−0.1493
K^+ [a]	−1863.4714	−599.0044	−1264.3172	−1264.3116	−0.1314
K^+ [b]	−1292.2569	−27.7878	−1264.3153	−1264.3117	−0.1355
Rb^+ [b]	−1287.9527	−23.5169	−1264.3104	−1264.3073	−0.1026
Cs^+ [b, c]	−1283.9469	−19.5326	−1264.3246	−1264.3209	−0.0799
Cs^+ [b, d]	−1283.9295	−19.5279	−1264.3065	−1264.3047	−0.0697

[a] calculated with an all-electron 6-31+G* basis sets. [b] calculated with the (electron-core potential) ECP-LanL2DZ basis set for the metal atom and the 6-31+G* basis set for the cryptand (whenever present). [c] Calculated for the *endo* $[Cs \subset 222]^+$ cryptate structure. [d] Calculated for the *exo* $[Cs \subset 222]^+$ cryptate structure. [e] $M^+(222)$: cryptate structure with cryptand 222 as ghost. [f] $222(M^+)$: cryptate structure with the alkali cation M^+ as ghost. [g] $222–M^+$: cryptate structure without M^+. [h] $\Delta E_{g,0}(M) = E_{g,0}([M \subset 222]^+) - E_{g,0}(222) - E_{g,0}(M^+(222)) - E_{g,0}(222(M^+)) + E_{g,0}(222 - M^+)$, where $E_{g,0}(222) = -1264.3300$ E_h is the energy of the isolated 222 cryptand in the gas-phase (geometry-optimized in the absence of cation).

All energies in E_h (1 E_h=2625.499 kJ mol^{-1}) and the values for $\Delta_{g,0}E(M)$ in kJ mol^{-1} are presented in Table 4.

Table 4 Internal energy changes $\Delta_{g,0}E$ (Table 3), thermal corrections $\Delta\Delta_{g,T}E$ and standard entropy contributions $-T\Delta_gS$ to the standard gas-phase Gibbs free energy of complexation $\Delta_gG°$ of the $[M \subset 222]^+$ cryptates at 298 K, Eq. (6)

Ion	$\Delta_{g,0}E$	$\Delta\Delta_{g,T}E$	$-T\Delta_gS°$	$\Delta_gG°$
Na^+ [a]	−392.0	9.2	47.0 (43.9)	−335.8
K^+ [a]	−345.0	7.9	46.4 (45.7)	−290.7
K^+ [b]	−355.7	8.0	46.5 (45.7)	−301.2
Rb^+ [b]	−269.4	6.3	46.6 (48.2)	−216.5
Cs^+ [b, c]	−209.7	4.1	44.8 (49.5)	−160.8

[a] Thermal corrections and standard entropy contributions calculated with an all-electron 6-31G basis sets. [b] Thermal corrections and standard entropy contributions calculated with the (electron-core potential) ECP-LanL2DZ basis set for the metal atom and the 6-31G basis set for the cryptand (whenever present). [c] Calculated for the *endo* $[Cs \subset 222]^+$ cryptate structure.

The purely translational contributions to the entropy term (Sackur-Tetrode equation) are also indicated between parentheses. All values in kJ mol^{-1}.

$[Na \subset 222]^+$ cryptate being the most stable of the series while the $[Cs \subset 222]^+$ cryptate is the least stable.

The standard absolute solvation free energies $\Delta_{sol}G^{\circ}_{abs}$ obtained from the MC simulations with thermodynamic integration for the alkali cations in water and in 80:20 (v/v) methanol:water solution are reported in Table 5. The calculated values in water are in good agreement with the experimental data [48], with errors comprised between 1.6 and 4.1%. Note that the corresponding absolute error is largely systematic (moderate dependence on the ion size) and certainly correlated with the use of an approximate form for the long-range electrostatic interactions in the simulations [45]. The free energies of transfer $\Delta_{trn}G$ from water to the methanol-water solution are also reasonably well reproduced compared to the experimental data [49]. However, the calculated results show that $\Delta_{trn}G$ increases as the ionic radius increases, which is not observed in the experimental data, which has the following order $Li^+ < Na^+ < K^+ \approx Cs^+ < Rb^+$, practically independent of the methanol:water ratio [49]. This might be explained considering that $\Delta_{trn}G$ is calculated as the difference between two large numbers of the same magnitude that yields a small number, and even small errors in the calculated absolute values can lead to large errors in the $\Delta_{trn}G$ values.

The final results for the relative free energies of complexation $\Delta\Delta_cG$ of the $[M \subset 222]^+$ cryptates in 80:20 (v/v) methanol-water solution for the alkali series M = Na, K, Rb and Cs, Eq. (4), are reported in Table 5, together with the corresponding gas phase contributions $\Delta\Delta_gG$ and solvation contributions $\Delta\Delta_{sol}G^{cry}$ and $\Delta\Delta_{sol}G^{ion}$, and with experimental data [29].

Based on the present quantum-chemical calculations (Table 4), the $[Na \subset 222]^+$ cryptate is the most stable in the gas phase while the stabilities of the successive cryptates decreases in the order Na > K >> Rb >> Cs. This decrease is correlated with the increase in the ionic radius of the corresponding monovalent ions [41]: 132, 165, 175 and 188 pm for Na^+, K^+, Rb^+ and Cs^+, respectively. Similar trends [20, 21] have been observed for the complexation of alkali cations with crown ethers in the gas phase. This gas-phase selectivity can certainly in part be explained by an increasing (closed-shell) overlap between the electron clouds of the cation and the cryptand molecule that destabilizes the complex (steric effect). However, inspec-

Table 5 Comparison between calculated and experimental standard absolute solvation free energies $(\Delta_{sol}G^{\circ}_{abs})$ of alkali cations in water and in 80:20 (v/v) methanol:water solution, and transfer free energies ($\Delta_{trn}G$) from water to the methanol-water mixture

Water	$\Delta_{sol}G^{\circ}_{abs}$	$\Delta_{sol}G^{\circ}_{abs}$	$\Delta_{sol}G^{\circ}_{abs}$
Ion	Calculated[a]	Experimental [48, 52]	Difference (%)
Na^+	−383.3	−375	−8.3 (2.2)
K^+	−313.7	−304	−9.7 (3.2)
Rb^+	−292.5	−281	−11.5 (4.1)
Cs^+	−262.2	−258	−4.2 (1.6)
Methanol-water mixture	$\Delta_{sol}G^{\circ}_{abs}$	$\Delta_{trn}G$	$\Delta_{trn}G$
Ion	Calculated[b]	Calculated	Experimental [49]
Na^+	−380.2	3.2	6.6
K^+	−307.5	6.2	7.0
Rb^+	−284.6	7.9	7.8
Cs^+	−251.9	10.4	6.9

[a] The free energy changes associated with the processes $Na^+ \rightarrow Na^0, Na^0 \rightarrow CH_4, CH_4 \rightarrow$ dummy are 401.70, −0.85 and −9.51 kJ mol^{-1}; the negative of the latter value can be compared with the experimental value for the standard hydration free energy of the methane molecule 8.28 kJ mol^{-1} [48, 52, 53]. [b] The free energy changes associated with the processes $Na^+ \rightarrow Na^0, Na^0 \rightarrow CH_4, CH_4 \rightarrow$ dummy are 395.32, −4.83 and −2.34 kJ mol^{-1}. [c] To calculate the standard absolute solvation free energies $\Delta_{sol}G^{\circ}_{abs}$ a contribution of 7.96 kJ mol^{-1} was added to the simulated results [45] to account for the compression work of an ideal gas from 1 bar (standard pressure) to 1 mol L^{-1} (standard concentration).

All values in kJ mol^{-1}

Table 6 Relative free energies of complexation $\Delta\Delta_c G$ for the alkali cryptates in 80:20 (v/v) methanol:water solution, Eq. (4), together with the corresponding gas-phase contributions $\Delta\Delta_g G$ and solvation contributions $\Delta\Delta_{sol}G^{ion}$ and $\Delta\Delta_{sol}G^{ion}$

Process	$\Delta\Delta_g G$	$\Delta\Delta_{sol}G^{cry}$	$\Delta\Delta_{sol}G^{ion}$	$\Delta\Delta_c G$ Calculated	Experimental [29]
$Na^+ \rightarrow K^+$	45.1	−8.0	72.7	−35.6	−14.1
$K^+ \rightarrow Rb^+$	84.7	−16.4	22.9	45.4	8.1
$Rb^+ \rightarrow Cs^+$	55.7	−3.9	32.8	19.0	24.3

All values in kJ mol^{-1}

tion of the partial charges attributed by the CHELPG analysis to the ion and oxygen atoms within the gas-phase cryptates (Table 1) also suggests that the amount of charge transfer decreases along the alkali series. Thus, the observed gas-phase selectivity might also be in part due to a reduced extent of delocalization of the ionic charge within the cryptate upon increasing the ionic radius (electronic effect).

When going from gas phase to the 80:20 (v/v) methanol: water solution, the relative stabilities of the alkali cryptates is affected by quantitative as well as qualitative changes (solvent effect), as previously observed in the case of the crown ethers [20, 21] and other cryptates [22, 23]. Based on the present calculation (Table 6), it is the $[K \subset 222]^+$ cryptate that is the most stable in solution, while the stability of the successive cryptates decreases in the order $K^+ >> Na^+ \approx Rb^+ > Cs^+$, which can be visualized in Fig. 2 that presents the relative equilibrium formation constants.

This trend agrees qualitatively well with the experimental results [24, 29], although the relative stability of the $[K \subset 222]^+$ cryptate is significantly overestimated and the

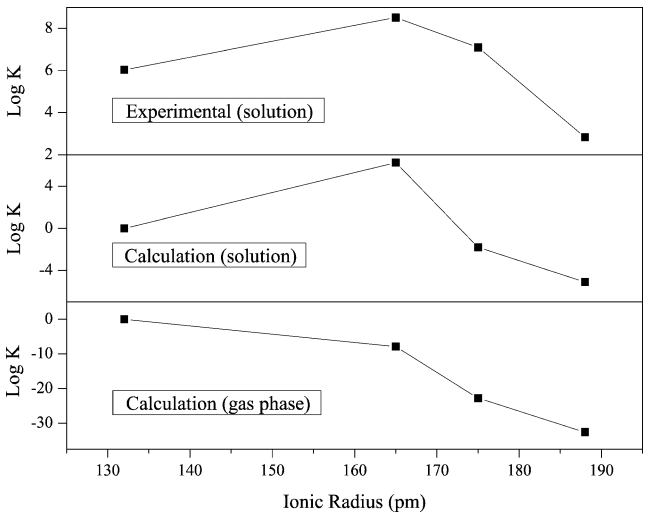

Fig. 2 Experimental [29] and calculated relative equilibrium constants for the $[M \subset 222]^+$ cryptates in gas phase and in methanol:water solution. The calculated values for the $[Na \subset 222]^+$ cryptates in gas phase and in solution are taken as zero to obtain the relative values

relative stability of the $[Rb \subset 222]^+$ is higher than that of the $[Na \subset 222]^+$ in contrast to the experimental results. These discrepancies are probably due to the quantum chemical calculations that used distinct and non-systematic basis sets for these ions. As a result, quantitative agreements would require systematic basis sets and inclusion of balanced correlation effects as well as relativistic corrections, which are probably not provided by the large core effective pseudo-potentials. However, it should be noted that these results are also related to the stability constants for the alkali cations within the 222 cryptand in an 95:5 methanol: water solution [50], even though this is not exactly the same volume fraction of methanol:water used in this work.

The dominant contribution to the solvent effect is the dessolvation penalty of the alkali ion, which increases in magnitude with decreasing ion size and is particularly large for the Na^+ cation. The solvation free energies of the cryptates are more weakly affected by the nature of the cation and increase moderately in magnitude with increasing cation size. This moderate dependence can easily be rationalized in terms of the Born model [51] of ionic solvation (all cryptates have the same net charge and nearly identical sizes). The slight increase in magnitude may be correlated with the higher partial atomic charges within the cryptates involving larger ions (Table 1). Based on the present results, the solvation-induced stability inversion between the $[Na \subset 222]^+$ and $[K \subset 222]^+$ cryptates can be attributed to: (i) a limited gas-phase stability difference (compared to the Na-Rb and, to a lesser extent, Rb-Cs pairs); (ii) a particularly large solvation free energy difference for the corresponding alkali cations (compared to the Na-Rb and Rb-Cs pairs). The above observations suggest that the influence of the solvent can be very significant but not easily predictable in the context of the molecular recognition process involving ionophores, and their use as models for more complex systems.

Conclusions

The molecular recognition process involved in the formation of alkali 222 cryptates was investigated by means of

gas-phase quantum-chemical calculations and explicit-solvent Monte Carlo free-energy calculations. The results suggest that the relative stabilities of the cryptates in solution are determined by the interplay between (at least) three types of effects: (i) steric effects (compression of large ions within the cryptand cavity); (ii) electronic effects (delocalization of the ionic charge onto the cryptand atoms); (iii) solvent effects (dominantly the ionic dessolvation penalty). Thus, these relative stabilities cannot be rationalized solely on the basis of a simple match or mismatch between the ionic radius and the cryptand cavity size, as has been suggested previously [24, 25]. The present calculations permitted to quantify the relative contributions of the gas-phase affinity and solvent effects to the stability of alkali 222 cryptates. The results underline in particular the key role played by the solvent (or solvent mixture) in establishing the selectivity of ionophores in solution, dominantly via the ion dessolvation contribution. In particular, since the electrostatic contribution to solvation is likely to be the leading effect, a change of the solvent (or solution) polarity may have a large impact on the selectivity along the alkali cation series.

The trends observed in the present study agree qualitatively well with experimental results [24, 29] and with previous molecular simulation studies of cryptates in pure water and pure methanol [22, 23]. Thus, the combined use of quantum-chemical calculations in the gas phase and classical atomistic simulations in solution appears to provide a practical and reliable approach to analyze relative ion-ligand binding affinities in solution.

Acknowledgements This work was partially supported by FAPESP, CAPES, CNPq, PADCT and CENAPAD-SP. ESL thanks FAPESP for the award of a fellowship.

References

1. Lehn JM (1995) Supramolecular chemistry: Concepts and perspectives. VCH, New York
2. Dobler M (1981) Ionophores and their structures. Wiley, New York
3. Lehn JM (1993) Science 260:1762–1763
4. Cram DJ (1988) Angew Chem - Int Ed Eng 27:1009–1020
5. Lehn JM (1978) Pure Appl Chem 50:871–892
6. Cram DJ, Cram JM (1974) Science 183:803–809
7. Kyba EP (1977) J Am Chem Soc 99:2564–2571
8. Rauwolf C, Straßner T (1997) J Mol Mod 3:1–16
9. Bell SEJ, McKervey MA, Fayne D, Kane P, Diamond D (1998) J Mol Mod 4:44–52
10. Puchta R, Seitz V, Hommes NvE, Saalfrank RW (2000) J Mol Mod 6:126–132
11. Dickert FL, Landgraf S, Sikorski R (2000) J Mol Mod 6:491–497
12. Puchta R, Clark T, Bauer W (2006) J Mol Mod 12:739–747
13. Pumera M, Rulíšek L (2006) J Mol Mod 12:799–803
14. Stryer L (1988) Biochemistry, 3rd edn. W. H. Freeman and Company, New York, p 967
15. Marrone TJ, Merz Jr KM (1995) J Am Chem Soc 117:779–791
16. Auffinger P, Wipff G (1991) J Am Chem Soc 113:5976–5988
17. Boudon S, Wipff G (1991) J Chim Phys 88:2443–2449
18. Troxler L, Wipff G (1994) J Am Chem Soc 116:1468–1480
19. Feller D (1997) J Phys Chem A 101:2723–2731
20. More MB, Ray D, Armentrout PB (1999) J Am Chem Soc 121:417–423
21. Glendening ED, Feller D, Thompson MA (1994) J Am Chem Soc 116:10657–10669
22. Auffinger P, Wipff G (1991) J Chim Phys 88:2525–2534
23. Wipff G (1992) J Coord Chem 27:7–37 Part B
24. Zhang XX, Izatt RM, Bradshaw JS, Krakowiak KE (1998) Coord Chem Rev 174:179–189
25. Martell AE, Hancock RD, Motekaitis RJ (1994) Coord Chem Rev 133:39–65
26. Solomons TWG (1992) Organic chemistry, 5th edn. Willey, New York, p 443
27. Galle M, Puchta R, Hommes NvE, van Eldik R (2006) Z Phys Chem 220:511–523
28. $[K \subset 222]^+$: Moras D, Metz B, Weiss R (1973) Acta Cryst B 29:383–388; $[Rb \subset 222]^+$ and $[Cs \subset 222]^+$: Moras D, Metz B, Weiss R (1973) Acta Cryst B 29:388–395; $[Na \subset 222]^+$: Moras D, Weiss R (1973) Acta Cryst B 29:396–399
29. Krakowiak KE, Zhang XX, Bradshaw JS, Zhu CY, Izatt RM (1995) J Incl Phenom 23:223–231
30. Chen Q, Cannell K, Nicoll J, Deaden DV (1996) J Am Chem Soc 118:6335–6344
31. McQuarrie DA (1976) Statistical Mechanics, 1st edn. HarperCollins Publishers, New York
32. Frisch MJ, Trucks GW, Schlegel HB, Gill PMW, Johnson BG, Robb MA, Cheeseman JR, Keith TA, Petersson GA, Montgomery JA, Raghavachari K, Al-Laham MA, Zakrzewski VG, Ortiz JV, Foresman JB, Peng CY, Ayala PY, Wong MW, Andres JL, Replogle ES, Gomperts R, Martin RL, Fox DJ, Binkley JS, Defrees DJ, Baker J, Stewart JP, Head-Gordon M, Gonzalez C, Pople JA (1995) Gaussian 94 (Revision D.1) Gaussian Inc, Pittsburgh PA
33. Hehre WJ, Radom L, Schleyer PvR, Pople JA (1986) Ab initio molecular orbital theory. Wiley, New York
34. Boys SF, Bernardi F (1970) Mol Phys 19:553–566
35. Hay PJ, Wadt WR (1985) J Chem Phys 82:299–310
36. Kollman P (1993) Chem Rev 93:2395–2417
37. Allen MP, Tildesley DJ (1997) Computer simulation of liquids. Clarendon Press, Oxford
38. Barker JA, Watts RO (1973) Mol Phys 26:789–792
39. Jorgensen WL (1998) OPLS force fields. In: Schleyer PvR (ed) The encyclopedia of computational chemistry, vol 3. Wiley, New York, p 1986
40. Breneman CM, Wiberg KB (1990) J Comp Chem 11:361–373
41. Huheey JE, Keiter EA, Keiter PL (1993) Inorganic chemistry: Principles and reactivity, 4th edn. Harper Collins, New York, p 114
42. Fuentealba P, Preuss H, Stoll H, Szentpály LV (1982) Chem Phys Lett 89:418–422
43. Jorgensen WL, Blake JF, Buckner JK (1989) Chem Phys 129:193–200
44. Freitas LCG (1991) Diadorim Program. Theoretical Chemistry Laboratory, Departamento de Química, UFSCar, São Carlos, SP, Brazil; Freitas LCG (1993) J Mol Struct: Theochem 101:151–158
45. Kastenholz MA, Hünenberger PH (2006) J Chem Phys 124:224501-1-20

46. Helgaker T, Jorgensen P, Olsen J (2000) Molecular electronic-structure theory, 1st edn. Wiley, New York, chapter 15
47. Soong L-L, Leroi GE, Popov AI (1992) J Inclusion Phenom 12:253–262
48. Marcus Y (1997) Ion properties, 1st edn. Marcel Dekker, New York, p 121
49. Kalidas C, Hefter G, Marcus Y (2000) Chem Rev 100:819–852
50. Lehn JM, Sauvage JP (1975) J Am Chem Soc 97:6700–6707
51. Born M (1920) Z Phys 1:45–48
52. Bem-Naim A (1987) Solvation thermodynamics. Plenum Press, New York
53. Freitas LCG, Botelho LF (1994) Quim Nova 17:489–495